Hyperpolarizabilities measured for interacting molecular pairs

E.A. Donley and D.P. Shelton
Physics Department, University of Nevada, Las Vegas, Las Vegas, NV 89154, USA

Received 22 July 1993; in final form 28 September 1993

Hyperpolarizability ratios for molecules have been measured with 0.1% accuracy, at $\lambda = 514.5$ nm, in the gas phase as a function of density. These measurements yield $\gamma(H_2)/\gamma(He) = 19.55 \pm 0.03$, $\gamma(Ar)/\gamma(H_2) = 1.668 \pm 0.002$ and $\gamma(N_2)/\gamma(H_2) = 1.283 \pm 0.001$ in the zero density limit. Pair interaction contributions, determined from the density dependence of γ, are larger than predicted assuming classical multipolar interactions, and of the opposite sign. Extrapolated to liquid density, the pair interaction contributions to γ are about as large as the isolated molecule contributions to γ for Ar and N_2.

1. Introduction

There have been many recent experimental and theoretical studies of the nonlinear optical properties of materials [1], and there has been a strong interplay between theory and experiment in the design of organic molecular nonlinear optical materials for applications. However, experimental measurements are generally made for condensed phase systems while theoretical calculations are generally made for isolated atoms or molecules. In the case of CH_3CN, where accurate gas phase and condensed phase measurements and ab initio calculations are available, it is found that the gas phase and ab initio results agree but the hyperpolarizabilities of the molecules in the condensed phase are 2 or 3 times larger, even after the usual local field corrections have been applied [2]. Different solvent environments have been shown to alter the measured hyperpolarizability of a molecule such as *p*-nitroaniline by a factor of two [3]. Although the effects of intermolecular interactions on the nonlinear optical properties of molecules appear to be large, these effects are not well studied or understood.

In order to study the effect of intermolecular interactions on molecular hyperpolarizabilities, we have made gas phase measurements of the second hyperpolarizabilities γ for He, H_2, N_2 and Ar at several gas densities. Intermolecular interactions will alter γ of the colliding pairs of atoms or molecules which are present at finite gas density, and the measurable effect will be a small deviation from linear density dependence for the nonlinear susceptibility of the gas. The analogous effect for the linear polarizability α is described by the second and higher refractivity virial coefficients [4]. In the case of small nonpolar molecules the second refractivity virial coefficient is small, the Clausius–Mossotti relation is quite accurate, and the values of α derived from gas phase and liquid phase measurements agree to within a few percent [5]. In the case of the hyperpolarizabilities, gas phase and liquid phase results appear to disagree strongly, so one may expect to find a measurable density dependence for hyperpolarizability in the gas phase even at low densities.

2. Experiment

Hyperpolarizability ratios were determined by means of electric-field-induced second harmonic generation (ESHG) with periodic phase matching, as previously described [6,7]. The beam of an argon-ion laser is weakly focused into the sample cell containing the gas under study, and the beam propagates along the midplane of a periodic array of pairs of cylindrical electrodes. Peak harmonic signal is obtained by adjusting the gas density to satisfy the periodic phase matching condition. The ratio of hyperpolarizabilities for two gases A and B is

determined from measurements made at phase match for each gas in turn,

$$\gamma_A/\gamma_B = (S^{1/2}/q\rho V)_A/(S^{1/2}/q\rho V)_B\,, \qquad (1)$$

where S is the measured harmonic photon flux, ρ is the gas density at phase match, V is the voltage applied to the electrodes, and $q \approx 1$ accounts for small systematic differences between the conditions for the two samples. Since phase match occurs at a fixed density for a given array periodicity and gas, four different electrode arrays were required to obtain measurements of γ_A/γ_B at four different gas densities. The array parameters and typical operating conditions are outlined in table 1, and the results of the measurements are summarized in table 2.

Refinements of previous technique and analysis were required in order to ensure accuracy at the 0.1% level for the measurements in table 2. Altogether about 200 triplets of measurements were made, with agreement between individual measurements close to their shot noise limit (range from $\pm 0.5\%$ for array No. 1 down to $\pm 0.1\%$ for array No. 4). The density of the high-purity gas (99.999%) was determined with accuracy better than 0.1% in all cases, from measurements of the gas pressure ($\pm 0.02\%$–0.08%) and temperature ($\pm 0.1\,^{\circ}C$), by means of the virial equation of state [8]. Statistical and calibration uncertainties each contribute about $\pm 0.07\%$ to the error bars on the final results. The stated uncertainties are treated as one standard deviation. The final results may be somewhat more accurate than the assigned error bars suggest, since the systematic uncertainties for the final results may have been too conservatively estimated.

Corrections for systematic effects on the harmonic signal enter through the factor q in eq. (1). The factor q is mainly a function of the refractive index n_ω [9] of the gas at phase match density, and is given by

$$q = (T_1^2 T_2)^{1/2} (F)^{1/2} (n_\omega^{\zeta-2} n_{2\omega}^{-1})^{1/2} \times (f_0 f_\omega^2 f_{2\omega})\,, \qquad (2)$$

where $f_\omega = \frac{1}{3}(n_\omega^2 + 2)$. Four distinct factors contribute to q. The first factor accounts for the Fresnel reflection losses at the surfaces of the entrance and exit windows. Only the gas-sample-dependent changes in the intensity transmission coefficients T_1 and T_2 for the entrance and exit windows need to be accurately accounted for (the windows are uncoated fused silica to make T calculable). The second factor accounts for the change in beam focusing inside the cell because of the lens induced in the entrance window by the gas pressure [10]. The factor F is evaluated in three steps for every experimental configuration: (i) the focal length of the entrance window as a function of gas pressure is obtained from the numerical solution for its mechanical and optical deformation [10], (ii) the changes in the laser beam propagation parameters due to the pressure-induced lens are computed, and (iii) the factor F is obtained as the ratio of the ESHG signals calculated by numerical integration of eq. (1) in ref. [6], for modified and unmodified laser beams passing through the electrode array. In the third factor, n_ω^ζ accounts for the change in beam focusing at the entrance window due to changes in gas refractive index, and is obtained by a calculation analogous to that for F (where $n - 1 \ll 1$ allows the result to be expressed in the form n^ζ, and typically $\zeta \approx 0.4$), while $n_\omega^{-2} n_{2\omega}^{-1}$ arises from rela-

Table 1
Parameters of electrode arrays used in these measurements. Each array consists of N pairs of cylindrical electrodes of diameter D. The electrodes are arranged in two rows and have longitudinal and transverse center-to-center spacing L, giving an array of overall length NL with interelectrode gap width $L-D$. The laser beam propagates in the narrow gap, down the long axis of the array. The signal and gas density at phase match is given for H_2 in the typical case in which a 3 W laser beam is focused to give a confocal parameter $z_0 = NL$, and $V = 3$ kV is applied to the electrode array

Array	L (mm)	D (mm)	N	$S(H_2)$ (cps)	$\rho(H_2)$ (mol m^{-3})
1	5.080	3.18	82	300	80.5
2	2.692	1.60	150	2300	152.4
3	2.032	0.76	200	3500	202.3
4	1.270	0.56	160	14000	323.5

Table 2
Measured hyperpolarizability and phase match density ratios for the gases He, H_2, N_2 and Ar, at $\lambda = 514.5$ nm ($\nu = 19430\ cm^{-1}$). The phase match density of the gas is inversely proportional to the polarizability dispersion $[\alpha(2\omega) - \alpha(\omega)]$. Gas pressures in these measurements are in the range 1–8 atm at $T = 298$ K, except for He where the range is 25–125 atm. The measured phase match density ratios show no significant density dependence (an increase by 0.01%–0.02% over this density range is predicted from measured refractive index virial coefficients [4])

	A	B	Array No. 1	Array No. 2	Array No. 3	Array No. 4
γ_A/γ_B	H_2	He	19.561±0.025	19.560±0.034	19.577±0.024	19.586±0.018
	Ar	H_2	1.6667±0.0029	1.6659±0.0012	1.6653±0.0012	1.6639±0.0011
	N_2	H_2	1.2814±0.0014	1.2818±0.0009	1.2811±0.0012	1.2798±0.0009
ρ_B/ρ_A	H_2	He	14.569±0.019	14.576±0.011	14.582±0.009	14.570±0.009
	Ar	H_2	1.3611±0.0007	1.3610±0.0007	1.3612±0.0007	1.3605±0.0007
	N_2	H_2	1.4613±0.0007	1.4612±0.0007	1.4612±0.0007	1.4607±0.0007

tions between optical field, polarization and power. The final factor contains the Lorentz local field factors f_ω. Since the phase match density for He gas is 15× larger than that for any of the other gases, the corrections are about an order of magnitude larger for He. The largest correction to γ is −0.8% for He gas with array No. 4 (−0.07%, −0.25%, +0.51%, −0.99% from each factor, respectively). The corrections for gases A and B tend to cancel in eq. (1), so the net correction to γ_A/γ_B is typically much less than 0.1%.

Several sources of potentially serious systematic errors have been eliminated at the 0.01% level of accuracy by careful experimental design and procedure. The effects of detector nonlinearity and coherent second harmonic background are eliminated by adjusting the electrode voltage V so that the ESHG signals from sample and reference gases are equal. The effects of drifts are eliminated by making measurements in triplets (e.g. ABA). The gas cell windows have a wedge angle between their surfaces which is large enough to eliminate "etalon" interference effects which would otherwise result in a modulation of the transmitted laser beam power with gas pressure and temperature. The laser beam must be made to remain in the electrode array midplane where the transverse gradient of the electrostatic field vanishes. This requires correct orientation of the wedge in the windows and critical mechanical alignment of the electrode array with respect to the axis to the windows. Since the tilted window surfaces enclose a prism of gas, there are small, unavoidable deflections of the laser beam in the symmetry plane of the electrodes due to changes in refractive index of the gas. The spectrometer and detector were adjusted to be insensitive to such beam deflections. The optical field was polarized parallel to the static field, and depolarization of the laser beam by the cell windows was kept at negligible levels by supporting the windows on optically polished seats. The extinction ratio of the complete cell between crossed polarizers was below 10^{-5} at all gas pressures. Filling the gas cell results in transient cell temperature changes of as much as 3°C because the low-pressure sample gas is obtained from a high-pressure gas supply. Thermal gradients in the gas result in beam deflection and lensing inside the electrode array. Relaxation of thermal gradients was accelerated by stirring the gas in the cell, and the approach to homogeneity could be monitored with a sensitivity of 0.01°C using the ESHG signal itself (the gas was not stirred during the final measurement) [11].

3. Results and discussion

Fig. 1 shows the hyperpolarizability ratios γ_A/γ_B plotted versus gas density. The present results agree with the best previous experimental results at this wavelength to within 0.5% [6]. The differences may be attributed to various small systematic errors present in previous work but eliminated in the present work. The lines through the data points in fig. 1 are weighted least-squares fits of a function linear in density, with the fit coefficients given in table 3. The zero density intercepts give the hyperpolarizability

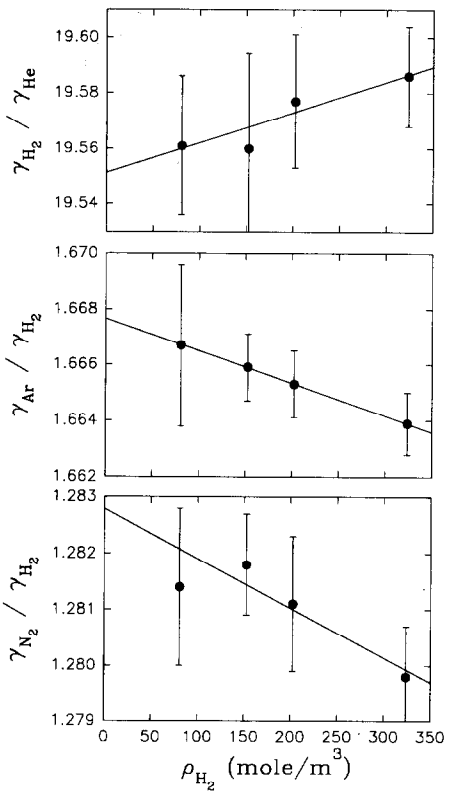

Fig. 1. Hyperpolarizability ratios $\gamma(H_2)/\gamma(He)$, $\gamma(Ar)/\gamma(H_2)$ and $\gamma(N_2)/\gamma(H_2)$ versus gas density $\rho(H_2)$, measured using four different electrode arrays (see tables 1, 2). As a result of the periodic phase matching condition, the ratios of gas densities $\rho(He):\rho(H_2):\rho(Ar):\rho(N_2)$ are very nearly the same for every array (see table 2). The ratio of hyperpolarizabilities for isolated molecules is determined from the zero-density intercept of the straight line fit through the data, while the slope of the line measures the effect of intermolecular interactions.

ratios of the isolated molecules and may be directly compared with the results of ab initio calculations. Thus, the current best ab initio results [12–17] are within 0.0%, +2.5% and +3.1% of the present experimental results for $\gamma(H_2)/\gamma(He)$, $\gamma(Ar)/\gamma(H_2)$ and $\gamma(N_2)/\gamma(H_2)$, respectively (see table 3). The present experimental result for $\gamma(H_2)/\gamma(He)$ confirms the high accuracy of the benchmark calculations of γ for the two-electron systems He [12] and H_2 [13].

The information about the effect of intermolecular interactions on the hyperpolarizabilities of pairs of molecules during collisions is contained in the slopes of the fitted lines in fig. 1. In order to interpret the experimental results we will make use of simple models. The simplest model represents the medium surrounding a molecule as a dielectric continuum [5], and results in the Lorentz local field factors appearing in eq. (2). The nonzero slopes of the lines in fig. 1 are a measure of the inadequacy of this approximation. This approximation does not accurately represent the classical multipolar interactions in a structured medium, and cannot represent the effects of the overlap of the wavefunctions of colliding molecules. The first problem may be dealt with by explicitly calculating the effects of nearby molecules while still representing the more distant molecules by a continuum [5]. The dominant multipolar interaction for atoms is described by the dipole–induced-dipole (DID) model, previously used to describe the effect of binary intermolecular interactions on the linear polarizability α [18,19]. In this model, each atom responds to the sum of the applied field and the field due to the dipole induced on the neighbouring atom. The self-consistent solution for the field and induced dipole may be expressed as a power series in R^{-3}, where R is the interatomic distance. Performing an isotropic average over all relative orientations of the interacting pair of atoms (assuming Kleinman symmetry for the atomic hyperpolarizability tensor), one may show that the apparent hyperpolarizability of an atom in the presence of a neighbour at a distance R is given by

$$\gamma(R)=\gamma[1+48(\alpha/4\pi\epsilon_0 R^3)^2]\,. \tag{3}$$

The relative hyperpolarizability increment $\Delta\gamma/\gamma=48(\alpha/4\pi\epsilon_0 R^3)^2$, where $\Delta\gamma(R)=[\gamma(R)-\gamma(\infty)]$, is 24× larger than the corresponding result for the linear polarizability $\alpha(R)$. Note that the leading terms, varying as R^{-3}, cancel in the isotropic average; but the shorter-range R^{-6} terms do not. The hyperpolarizability measured for atoms in a gas of number density ρ is obtained by averaging $\gamma(R)$ over the thermal distribution of interatomic distances R,

$$\gamma(\rho)=\gamma\left(1+\rho\int_0^\infty 4\pi R^2\,\mathrm{d}R\,g(R)48(\alpha/4\pi\epsilon_0 R^3)^2\right)$$

$$=\gamma(1+b\rho)\,, \tag{4}$$

where $g(R)=\exp[-U(R)/kT)]$ is the radial pair

Table 3
Measured and calculated values of the zero intercept $(\gamma_A/\gamma_B)_0$ and slope $b(AB)$ are compared. The measured values come from the least-squares fit of eq. (5) to the data in table 2 (see fig. 1). The calculated values of $(\gamma_A/\gamma_B)_0$ are obtained using the results of ab initio calculations of γ for ESHG at $\nu = 19430\ cm^{-1}$. Eq. (6) and the results for b in table 4 are used to calculate values of $b(AB)$ for the DID model

A	B	$(\gamma_A/\gamma_B)_{0,exp}$	$(\gamma_A/\gamma_B)_{0,calc}$	$b(AB)_{exp}$ $(10^{-6}\ m^3\ mol^{-1})$	$b(AB)_{calc}$ $(10^{-6}\ m^3\ mol^{-1})$
H_2	He	19.551±0.029	19.550 [a,b]	+5.6±6.2	−2.1
Ar	H_2	1.6677±0.0020	1.711 [b,c]	−7.0±5.0	+4.5
N_2	H_2	1.2828±0.0013	1.324 [b,d]	−6.9±4.6	+3.4

[a] $\gamma(He) = 47.946$ atomic units (1 au = $6.235377 \times 10^{-65}\ C^4\ m^4\ J^{-3}$) includes explicit reduced mass correction [12].
[b] $\gamma(H_2) = \gamma^{cvR} = 937.3$ au from $\gamma^e(H_2) = 945.4$ au [13], $\gamma^v(H_2) = -7.43 - 0.13 = -7.56$ au (fundamental + overtones), and $\gamma^R = -0.38$ au (quantum expressions for γ^{vR} given by eqs. 9–11 of ref. [6], evaluated using J-dependent Raman polarizability matrix elements [14] scaled to $\lambda = 514.5$ nm [15]).
[c] $\gamma(Ar) = 1604$ au from CCSD(T) static result and MP2 dispersion curve [16].
[d] $\gamma(N_2) = 1241$ au from CCSD(T) static result and SCF dispersion curve [17].

distribution function and $U(R)$ is the interatomic potential.

The calculated value of the coefficient b which describes the density dependence of $\gamma(\rho)$ within the binary DID approximation is given in table 4 for each of the molecules in the present study [20,21]. For comparison, the local field factor appearing in eq. (2) has been expanded as a power series in density, and the coefficient c which describes its linear density dependence is also given in table 4. The coefficients b and c describing the DID and local field corrections at low density are about the same size. The calculation of the classical multipolar interactions could be made more accurate by taking account of the following refinements: (i) more accurate intermolecular potential functions, (ii) correct values of independent tensor components of γ for each molecule, (iii) including effects of permanent quadrupole moments of the H_2 and N_2 molecules and possibly higher-order response tensors, (iv) including fluctuations in the moments which give a quantum correction to DID at this order [18,19]. However, the results given in table 4 are sufficient for the present purpose. A crude extrapolation of binary interactions to liquid density, while it cannot be expected to give accurate results for the properties of

Table 4
Pair polarizability estimated using the DID model (see eqs. (3,4)). The Lennard-Jones 6–12 form, $U(R) = 4\epsilon[(R/\sigma)^{-12} - (R/\sigma)^{-6}]$, has been assumed for the intermolecular potential. The value of $(\Delta\gamma/\gamma)_{R=\sigma}$ gives an estimate of the maximum change in $\gamma(R)$ during a collision. Averaging over the R distribution for molecular pairs in a gas of density ρ gives the density dependence of the measured hyperpolarizability, $\gamma(\rho)/\gamma = 1 + b\rho$. For comparison, the density dependence of the local field correction factor has been expressed in the same form, $[f_0 f_\omega^2 f_{2\omega}] = 1 + c\rho$

Gas	α [a] $(10^{-40}\ C^2\ m^2\ J^{-1})$	σ [b] (nm)	ϵ/k [b] (K)	$(\Delta\gamma/\gamma)_{R=\sigma}$ [c]	b [d] $(10^{-6}\ m^3\ mol^{-1})$	c [e] $(10^{-6}\ m^3\ mol^{-1})$
He	0.230	0.257	11	0.00714	0.46	2.10
H_2	0.92	0.30	40	0.0449	4.59	8.52
Ar	1.85	0.343	122	0.0815	12.43	17.13
N_2	1.97	0.366	97	0.0629	11.67	18.15

[a] From ref. [20], at $\lambda = 632.8$ nm.
[b] Ref. [21].
[c] From eq. (3).
[d] By numerical integration of eq. (4).
[e] From $c = \partial(f_0 f_\omega^2 f_{2\omega})/\partial\rho$, where $f_\omega = \frac{1}{3}(n_\omega^2 + 2)$ and $n_\omega = 1 + (N_A\alpha_\omega/2\epsilon_0)\rho$.

the liquid, does indicate that the effects of intermolecular interactions on γ can be large. Extrapolated to liquid density, the binary DID contribution in eq. (4) is 1%, 16%, 34% or 43% of the individual molecule contribution for He, H_2, N_2 or Ar, respectively. For larger, more strongly interacting molecules it is quite plausible that multipolar interactions could increase the hyperpolarizability by a factor of 2 or 3 at liquid density.

There is a slight complication in the comparison of the theoretical and experimental results which arises because ratios γ_A/γ_B are measured rather than γ_A and γ_B separately, so that the linear function fit to the data has the form

$$\gamma_A/\gamma_B = (\gamma_A/\gamma_B)_0[1+b(AB)\rho(H_2)] . \quad (5)$$

The relation between the experimentally determined slope $b(AB)$, and the coefficients b_A and b_B for molecules A and B calculated using eq. (4) and given in table 4, is

$$b(AB) = (b_A - b_B\rho_B/\rho_A)(\rho_A/\rho_C) , \quad (6)$$

where $C = H_2$. This relation holds since the measured density ratio for each gas pair is nearly constant, and since H_2 is common to all the measurements (see table 2). The measured and calculated values of $b(AB)$ are compared in table 3. The measured and calculated slopes agree in magnitude, but they are of opposite sign.

This discrepancy may be resolved if there is an additional contribution to $\gamma(R)$ which is twice as large as DID and of the opposite sign, such as a large but short-range "electron overlap" contribution. Support for this notion comes from studies of the pair polarizability $\alpha(R)$. Negative electron overlap contributions to $\alpha(R)$ are well established from experimental and theoretical results for the dielectric and refractivity virial coefficients of the noble gases [4, 18]. From the observed refractivity virial coefficients one may estimate that the electron overlap contributions to $\alpha(R)$ are about $-8\times$DID for He, $-3\times$DID for Ne, and about $-0.6\times$DID for H_2 and N_2 [4]. That the hyperpolarizability is very sensitive to overlap of the tails of the electronic wavefunctions of two molecules is suggested by the large electron correlation effects and the high sensitivity to diffuse basis functions seen in ab initio calculations of γ for single molecules. However, there have been few quantum mechanical calculations of the pair hyperpolarizability relevant to molecular collisions in gases [22,23]. The most pertinent results are those from the semi-empirical calculations of $\gamma(R)$ for He and Ne [22]. The calculated increment $\Delta\gamma(R)$ varies approximately as R^{-6} at long range, and is $-5\times$DID for He and $-2\times$DID for Ne. These results are consistent with electron overlap contributions to $\gamma(R)$ which are about $-2\times$DID, and which would account for the density dependence of γ measured in the present experiments, but further ab initio calculations are needed for quantitatively accurate predictions. Such quantum calculations of $\gamma(R)$ for molecular pairs will give the sum of the multipolar and electron overlap contributions. The distinction between these contributions is that the latter cannot be expressed in terms of the electrical response properties of the isolated molecules. For larger molecules, both the relative magnitude and sign of multipolar and electron overlap contributions to the hyperpolarizabilities are open questions.

4. Conclusion

One may draw several conclusions about hyperpolarizabilities of small molecules from this study. First, ab initio quantum chemical calculations are able to produce quantitatively accurate values of the hyperpolarizabilities of isolated atoms and molecules, as evidenced by the 0.1% agreement between theory and gas phase measurements for H_2 and He, and the better than 10% agreement for Ar and N_2. Second, reliable determinations of the hyperpolarizabilities of isolated molecules from measurements of the nonlinear susceptibility of a molecular liquid or solid should not be possible unless short-range intermolecular interactions as well as local field factors are taken into account. Third, the classical multipolar interactions between molecules and the changes in the molecular wavefunction during a collision both make comparable contributions to the hyperpolarizabilities of interacting molecules.

References

[1] D.M. Burland, ed., Special Issue on Nonlinear Optics, Chem. Rev., in press;
M. Ratner, ed., Special Issue on Molecular Nonlinear Optics, Intern. J. Quantum Chem. 43 (1992) 1;
C.M. Bowden and J.W. Haus, eds., Special Issue on Nonlinear-Optical Properties of Materials, J. Opt. Soc. Am. B 6 (1989) 562.

[2] M. Stähelin, C.R. Moylan, D.M. Burland, A. Willetts, J.E. Rice, D.P. Shelton and E.A. Donley, J. Chem. Phys. 98 (1993) 5595;
A. Willetts and J.E. Rice, J. Chem. Phys. 99 (1993) 426.

[3] M. Stähelin, D.M. Burland and J.E. Rice, Chem. Phys. Letters 191 (1992) 245.

[4] H.J. Achtermann, J.G. Hong, G. Magnus, R.A. Aziz and M.J. Slaman, J. Chem. Phys. 98 (1993) 2308;
H.J. Achtermann, G. Magnus and T.K. Bose, J. Chem. Phys. 94 (1991) 5669;
A.D. Buckingham and C. Graham, Proc. Roy. Soc. A 337 (1974) 275;
A.D. Buckingham, Trans. Faraday Soc. 52 (1956) 747.

[5] C.J.F. Böttcher, Theory of electric polarization (Elsevier, Amsterdam, 1973).

[6] D.P. Shelton, Phys. Rev. A 42 (1990) 2578.

[7] V. Mizrahi and D.P. Shelton, Phys. Rev. A 32 (1985) 3454;
D.P. Shelton and A.D. Buckingham, Phys. Rev. A 26 (1982) 2787.

[8] J.H. Dymond and E.B. Smith, The virial coefficients of pure gases and mixtures (Clarendon Press, Oxford, 1980);
W. Duschek, R. Kleinrahm, W. Wagner and M. Jaeschke, J. Chem. Thermodyn. 20 (1988) 1069;
T.J. Quinn, Temperature (Academic Press, New York, 1990).

[9] K.-H. Hellwege and A.M. Hellwege, eds., Landolt-Börnstein Series, Zahlenwerte und Funktionen, Band II, Teil 8 (Springer, Berlin, 1962);
P.J. Leonard, Atom Data Nucl. Data Tables 14 (1974) 21.

[10] D.P. Shelton, Rev. Sci. Instrum. 63 (1992) 3978.

[11] D.P. Shelton and E.A. Donley, Rev. Sci. Instrum. 64 (1993) 2399.

[12] D.M. Bishop and J. Pipin, J. Chem. Phys. 91 (1989) 3549.

[13] D.M. Bishop, J. Pipin and S.M. Cybulski, Phys. Rev. A 43 (1991) 4845.

[14] R.J. LeRoy and C. Schwartz, U. Waterloo Chemical Physics Research Report CP-301R (1987).

[15] D.M. Bishop and L.M. Cheung, J. Chem. Phys. 72 (1980) 5125.

[16] J.E. Rice, J. Chem. Phys. 96 (1992) 7580;
J.E. Rice, P.R. Taylor, T.J. Lee and J. Almlöf, J. Chem. Phys. 94 (1991) 4972.

[17] H. Sekino and R.J. Bartlett, J. Chem. Phys. 98 (1993) 3022.

[18] P. Dacre, Mol. Phys. 45 (1982) 1;
P. Dacre, Mol. Phys. 45 (1982) 17.

[19] A.D. Buckingham and C. Graham, Proc. Roy. Soc. A 337 (1974) 275.

[20] M.P. Bogaard and B.J. Orr, in: International review of science, physical chemistry, molecular structure and properties, Ser. 2, Vol. 2, ed. A.D. Buckingham (Butterworths, London, 1975) p. 149.

[21] T.M. Reed and K.E. Gubbins, Applied statistical mechanics (McGraw-Hill Kogakusha, Tokyo, 1973).

[22] M.G. Papadopoulos and J. Waite, Chem. Phys. Letters 135 (1987) 361.

[23] J.D. Augspurger and C.E. Dykstra, Intern. J. Quantum Chem. 43 (1992) 135.